ESTIMATING THE PROMPT FRACTION OF IN-CORE FLUX DETECTORS AND VALIDATING THEIR DYNAMICS IN POWER RUNDOWN MEASUREMENTS

O. Glöckler D. Cooke, G. Czuppon, K. Kapoor

Reactor Safety and Operational Analysis Department
Nuclear Technology Services, Ontario Hydro Nuclear
700 University Avenue, H11-E26, Toronto, Ontario M5G 1X6

INTRODUCTION

Power rundown tests of self-powered in-core flux detectors (ICFDs) are performed on a regular basis during planned reactor trips to confirm the compliance of ICFD response dynamics with design conditions. Time series of ICFD and ion chamber signals used in the SDS and RRS sytems are recorded simultaneously during the reactor trip and analyzed off-line. The linear output signals of ion chambers serve as 100% prompt reference signals.

The paper describes the methodology and some results of recent power rundown tests aimed at (1) estimating the effective prompt fraction (EPF) of the in-core flux detectors, (2) assessing the spatial distribution and effectiveness of the trip mechanism (drop of shut-off rods or poison injection), and (3) determining the accuracy and the limiting factors of the above EPF estimation. Anomalies in the dynamics of ICFDs and ion chambers, as well as, in the shut-off mechanism can be detected by analyzing the recorded transient curves.

DATA ACQUISITION

Multi-channel PC-controlled analog data acquisition hardware and signal processing software have been developed and regularly used in station rundown measurements. The custom-built signal conditioning and data acquisition hardware includes the following components: (1) multi-channel isolation (buffer) amplifiers for isolating the data acquisition system from station instrumentation, and (2) a PC-based multi-channel signal sampling (analog-to-digital conversion) with selectable sampling frequencies, filters, amplifiers and DC-offset units. Typically, 16-channel measurements are carried out at a sampling frequency of 50 or 100 Hz. Procedures for safely connecting analog station signals from their amplifier's test outputs to the data acquisition hardware have been established. The same hardware system is used in the reactor noise measurements of ICFDs, ion chambers, pressure, flow and temperature signals. Results of Ontario Hydro's noise analysis program have been reported in [1,2].

The analog voltage signals are directly connected to the isolated input of the multi-channel data acquisition system while the given safety channel is rejected. After the signal connection is made, the safety channel is tested and reset. The recording of the analog detector signals starts half an hour before the reactor shutdown and continues for 12-13 hours after the trip. The digitized multi-channel data are stored in files and analyzed off-line. Note that the digital output of ROP/NOP computers cannot be used for ICFD prompt fraction estimations, because the ROP/NOP data acquisition system does not meet the following requirements: (1) high sampling frequency (50-100 Hz), (2) simultaneous sampling of multi-channel analog signals, (3) inclusion of ion chamber linear output and trip marker signals.

A new portable data acquisition system has been developed in AECL Chalk River Laboratories, which will eventually replace the current system and will transfer the technology to the stations [3]. In the present configuration, the new system consists of two identical data acquisition units. Each unit is capable of sampling 16 signals simultaneously at a maximum sampling frequency of 2.4 kHz with 16-bit ADC resolution. The two units have optically isolated inputs, and they can be run in synchronized modes. The built-in analysis software offers a user friendly access to statistical calculations and graphical presentation of results. A power rundown software application is under development.

VALIDATING IN-CORE FLUX DETECTOR DYNAMICS

The primary objective of the rundown test is to confirm the functionality and dynamic response of in-core flux detectors and their amplifiers in operator initiated reactor trips by cross checking detector response signals. Reactor rundown tests can be performed during planned reactor trips for a limited number of ICFD detectors and ion chambers. The recorded response signals can also be used to estimate the effective prompt fractions (EPF) of ICFDs.

The following formula is used to calculate the effective prompt fraction, p:

$$p = \left(1 - \frac{\overline{V_D(t_1,t_2)} - V_B}{\overline{V_D(0)} - V_B}\right)\left(1 - \frac{\overline{V_{ICH}(t_1,t_2)} - V_{B'}}{\overline{V_{ICH}(0)} - V_{B'}}\right)^{-1} \tag{1}$$

where

$$\overline{V_D(t_1,t_2)} = \frac{1}{(t_2-t_1)}\int_{t_1}^{t_2} V_D(t)\,dt$$

$$\overline{V_{ICH}(t_1,t_2)} = \frac{1}{(t_2-t_1)}\int_{t_1}^{t_2} V_{ICH}(t)\,dt$$

and

- $V_D(t)$ and $V_{ICH}(t)$ are the recorded voltage signals of the ICFD and the linear output of the ion chamber, respectively,
- $\overline{V_D(0)}$ and $\overline{V_{ICH}(0)}$ are the averaged signal values measured before the trip,
- V_B and $V_{B'}$ are the zero-power voltage output of the ICFD and ion chamber signals (zero off-set). In the Darlington units, the ICFD signals and the linear output of the ion chamber amplifier give a nominal value of $V_B = 0.5$ volt at zero power level, and
- t = - 0.4 sec is marked by the Trip Marker signal, and $t_1 = 2.5$sec, $t_2 = 3.5$sec.

A detailed derivation of Equation (1) is given in Appendix A.

The ion chambers are assumed to record the power change accurately despite their out-of-core position. The Effective Prompt Fraction is determined by assuming that for times greater than 1.0 sec after the trip the ion chambers reflect the magnitude of the step change in the neutron flux, and the ion chamber signal provides a record of the average neutron flux response throughout the reactor power rundown.

SDS1-INITIATED RUNDOWN TESTS

Rundown measurements from 60% of F.P. are performed regularly in Darlington before scheduled outages [4,5,6]. In the SDS1-induced rundown test in Darlington Unit 1, the calculated prompt fractions of channels F and B vertical Inconel ICFDs had an average value of 104%, while the channel J horizontal Platinum-clad ICFDs had an average value of 91%. In the SDS1-induced trip test, the response curves of both vertical and horizontal ICFDs showed a clear top-to-bottom spatial dependency (delay), in correlation with the insertion of the shut-off rods:

After the initiation of the SDS1 trip, all signals remained at their pre-trip levels in the first 360 msec. After this initial 360 msec deadtime, all channel B and F ICFDs departed from their pre-trip values within an additional interval of 180 msec. First, the top ICFDs started decreasing, then the lower ICFDs. This time interval was shorter for channel J ICFDs, only 120 msec, because of the shorter vertical distances between the uppermost and lowermost horizontal ICFDs in channel J. The first signal which reached the 50% level of its pre-trip value was the uppermost ICFD in channel F, VFD19-1F, 690 msec after trip initiation. It was followed by the ICFDs in channel B in the uppermost zones (zone 3 and 10 ICFDs), which reached the 50% level of their pre-trip value approx. 700 msec after trip initiation (see Figure 1). Zone ICFDs at elevation zone 1, 6, 8 and 13 reached their 50% level at the same time, 805 msec after the trip. They were followed by zone 4 and 11 ICFDs at 910 msec, by the RRS-B ion chamber at 980 msec, by zone 2, 7, 9 and 14 ICFDs at 990 msec, and finally by zone 5 and 12 ICFDs at 1060 msec, after trip initiation. The lowermost ICFDs of channel F reached the 50% level last, at 1150 msec.

The horizontal SDS2-J ICFDs displayed a similar pattern of vertical time delays. The top ICFDs in HFD2 started responding to the trip 120 msec earlier than the bottom ICFDs in HFD12, HFD13, HFD14. Also, the top ICFDs reached the 50% level 400 msec earlier than the bottom ICFDs. In channel F, the maximum top-to-bottom time difference measured between the first and the last responding ICFDs in reaching the 50% level was approx. 460 msec (between VFD19-1F and VFD1-4F). In channel B, this maximum difference was 360 msec, between VFD27-1B in zone 10 and VFD1-3B in zone 5.

In a typical SDS1-trip, all signals go down from their pre-trip values to a low level ($\approx$ 10%) within a 1 sec interval. ICFDs at the same elevation had similar response curves to SDS1-trip (see Figure 1). This observation can be used to identify possible degradation of ICFDs or shut-off rods.

In-service and spare coiled Platinum ICFDs of Pickering-B are also regularly tested in SDS1-initiated trips starting from 100% of full power [7]. Rundown measurements were also used in the recent commissioning of new HESIR in-core flux detectors installed in Pickering-B Unit 6 in March 1996. Response signals of all SDS1/SDS2 HESIR in-core flux detectors and SDS1/SDS2 ion chambers to an SDS1-induced trip from 60% of F.P. were recorded and analyzed off-line. The effective prompt fractions of all ICFDs, estimated from the measured signals, were found to be above 90%. Detailed results of the rundown test are given in [8]. Similar rundown measurements are planned for the commissioning of new HESIR ICFDs to be used in the SDS-E system of Pickering-A units.

SDS2-INITIATED RUNDOWN TESTS

In the SDS2-induced rundown test in Darlington Unit 2 the average prompt fraction of channel F vertical Inconel ICFDs was 102%, while the channel J horizontal Platinum-clad ICFDs had an average value of 89%. In a similar SDS2-trip in Unit 4, the channel J horizontal ICFDs had an average value of 88%. The derived prompt fractions of channel J ICFDs in Unit 4 is given in Table 1 of Appendix B.

After the initiation of an SDS2 trip, all signals remain at their pre-trip levels in the first 400-420 msec. The first signals which reach the 50% level of their pre-trip values are the SDS2 ion chambers, typically 500-520 msec after trip initiation. They are followed by the southernmost ICFDs, which reached the 50% level of its pre-trip value 520-540 msec after trip initiation. The northernmost ICFDs were the last in reaching the 50% level (640-670 msec). The time delays of channel J ICFDs measured in Unit 4 are listed in Table 2 of Appendix B. The corresponding normalized rundown signals are shown in Figure 2. Similar SDS2-initiated rundown tests are planned in Darlington units 1, 2 and 3 on April 27-30, 1997.

In the SDS2-induced trip test, the response curves of both vertical and horizontal ICFDs displayed a time delay along the south-to-north line, following the pattern of the poison propagation inside the injection nozzles. This indicates that the poison propagation inside the injection nozzle is the main source of time delays, as opposed to the poison propagation in the moderator. The south-to-north propagation of poison inside the nozzle, causing delays in ICFD response, can be looked at as the insertion of a set of "horizontal shut-off rods", over a time period of approx. 100 msec. The maximum south-to-north time difference measured between the first and the last responding ICFDs was approx. 120-130 msec. In SDS2-trips all signals go down from their pre-trip values to a low level ($\approx$ 10%) within a 400 msec interval.

The eight poison injection nozzles penetrate the calandria on the south side. According to the design manual, 47.5 liters of poison per nozzle is injected in approx. 300 msec. Results of a simple model calculation shows, that it takes approximately 100 msec for the poison to reach the north end of the injection nozzle, that is, poison injection at the north end of the nozzle starts 100 msec later (it takes 100 msec to force the unpoisoned D2O out of the nozzle, or using the above analogy, to drive the "horizontal shut-off rods" in). During this 100 msec interval, 8 liters of poison per nozzle has been injected already in the south side of the calandria (64 liters for 8 nozzles). The ICFD measurement data support these results by showing (1) a clear south-to-north spatial dependency in response time, and (2) a maximum time difference of 130 msec in ICFD responses.

The SDS2-initiated rundown test in Unit 2 showed that the response of a horizontal ICFD (AF3J HFD2-RE3J) was slower than its expected value by approximately 40 msec. The nornalized rundown response curves are shown in Figure 3. The ICFD noise measurement performed at steady-state full power before the rundown test gave the same result. The 40 msec extra response time was derived from the noise signatures (APSD, coherence and phase functions) of ICFDs located in the same horizontal detector tube, measured at the fundamental vibration frequency of detector tube HFD2, 4.1 Hz. The same detectors in Units 1 and 3 showed normal neutron noise patterns in similar measurements.

NOISE ANALYSIS BASED VALIDATION OF DYNAMICS

The dynamics of ICFD and ion chamber signals can be also validated in reactor noise measurements performed at full-power steady-state operation. The technique is based on the measurement and analysis of the small fluctuations (noise) of detector signals. The derived multi-channel frequency dependent statistical functions are very sensitive to incipient failures in the dynamics of detectors and reactor processes. Noise analysis is applied in solving a wide variety of station problems in Ontario Hydro's CANDU reactors [1,2]. The data acquisition system, described in Section 2, is also extensively used in the reactor noise measurements of ICFDs, ion chambers, pressure, flow and temperature signals. The advantage of the noise analysis based validation of ICFD dynamics is that it is a non-intrusive passive technique, which can be performed any time between outages (rundown tests). Once the ICFD noise signatures are calibrated to the results of the reactor rundown test or the ion chamber noise, changes in the prompt fraction can be detected by noise analysis any time. Therefore, noise-based monitoring of detector performance can reduce the need for further rundown tests.

ACKNOWLEDGEMENTS

The rundown measurements were performed in Pickering-B and Darlington units with an active support of plant personnel. In particular the authors would like to acknowledge the contribution of A. Campbell, M. Tulett, R. Vilkko, D. Williams of PNGS-B; F. Amantea, F. Dermarkar, E. Sadok, M. Ramphal, M. Wightman of DNGS; and V. Ton of RSOAD, NTS.

REFERENCES

[1] O. Glöckler, M.V. Tulett, "Application of Reactor Noise Analysis in the CANDU Reactors of Ontario Hydro," IMORN-25, Raleigh NC, June 13-15, 1994. Progress in Nuclear Energy, Vol. 29, No. 3/4, pp. 171-191.

[2] O. Glöckler, M.V. Tulett, "Development and Application of Noise Analysis in CANDU Reactors: Ontario Hydro's Experience Gained in the Past Three Years," 7th Symposium on Nuclear Reactor Surveillance and Diagnostics, SMORN-VII, Avignon, France, June 19-23, 1995.

[3] S.T. Craig et al., "Portable System for Noise Data Acquisition", 7th Symposium on Nuclear Reactor Surveillance and Diagnostics, SMORN-VII. Avignon, France, June 19-23, 1995.

[4] O. Glöckler, K. Kapoor, G. Czuppon "Effective Prompt Fractions of In-Core Flux Detectors Derived from SDS1-induced Power Rundown Test of Darlington Unit 1 on August 28, 1995," Rep. RND-Q2-Rev.3, February, 1996.

[5] O. Glöckler, K. Kapoor, G. Czuppon "Effective Prompt Fractions of In-Core Flux Detectors Derived from SDS2-induced Power Rundown Test of Darlington Unit 2 on November 18, 1995," Rep. RND-R1-Rev.3, February, 1996.

[6] O. Glöckler, K. Kapoor, G. Czuppon "Effective Prompt Fractions of In-Core Flux Detectors Derived from SDS2-induced Power Rundown Test of Darlington Unit 4 on August 23, 1996," Rep. RND-T2-Rev.1, October, 1996.

[7] O. Glöckler, K. Kapoor, G. Czuppon, R. Vilkko "Effective Prompt Fractions of In-Core Flux Detectors Derived from SDS1-induced Power Rundown Test of Pickering-B Unit 8 on September 17, 1993," PB-IR-63700-5, 1997.

[8] O. Glöckler, K. Kapoor, G. Czuppon, R. Vilkko "Effective Prompt Fractions of HESIR In-Core Flux Detectors Derived from SDS1-induced Power Rundown Test of Pickering-B Unit 6 on March 18, 1996," PB-IR-63700-30, 1997.

RRS CHANNEL B RUNDOWN SIGNALS – 1 sec scale

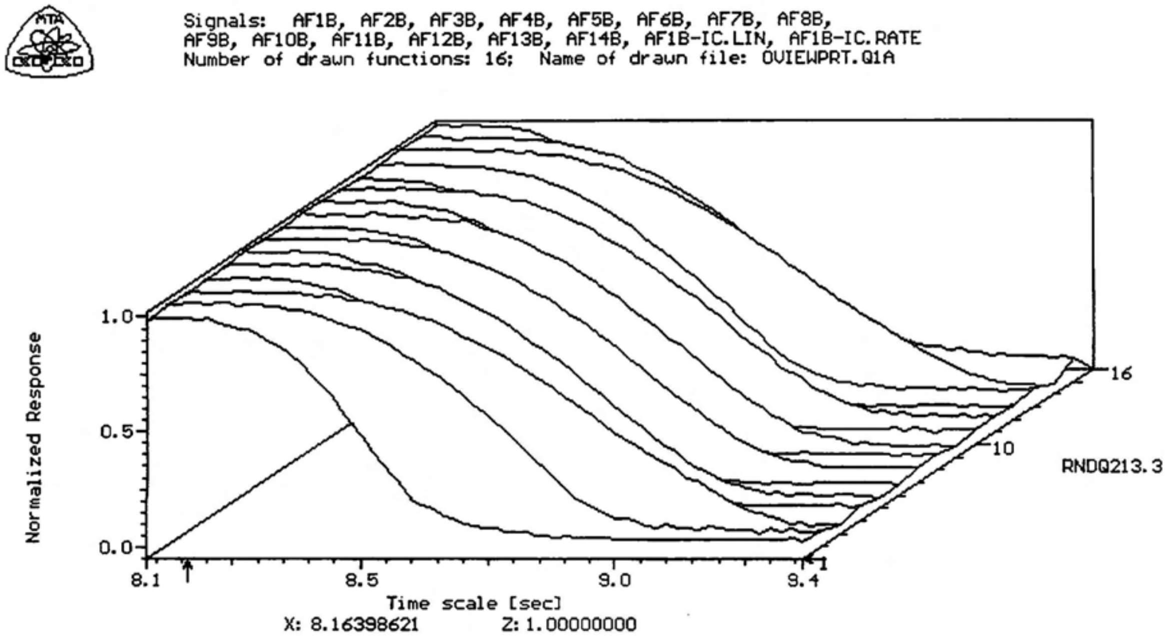

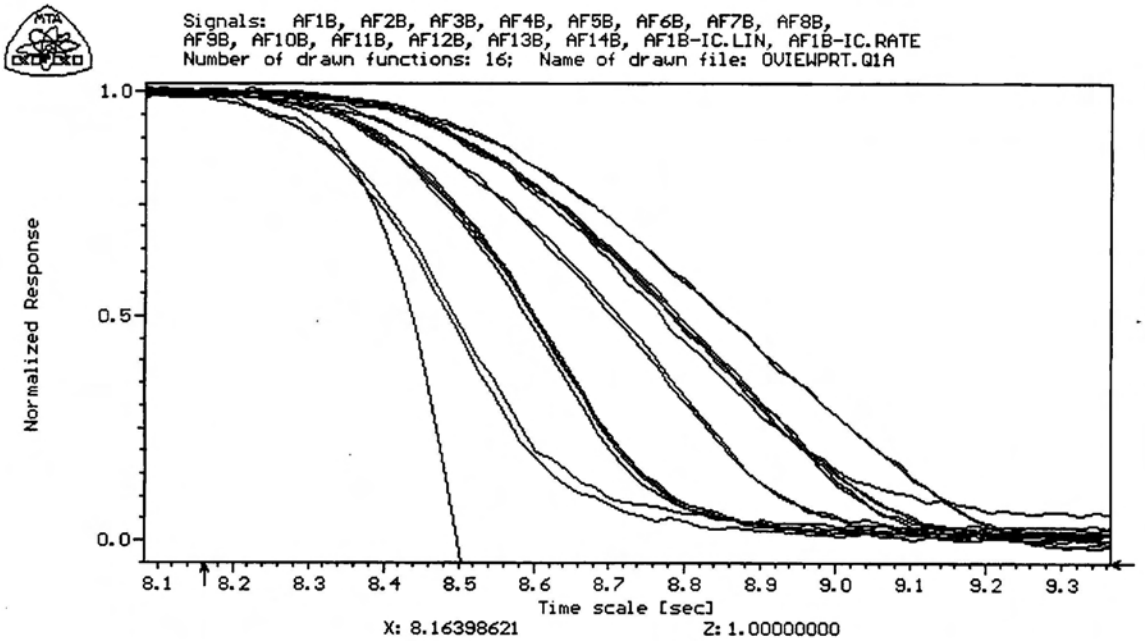

Figure 1. Rundown response signals of RRS-B ICFDs (AF-1B through AF14B),
RRS-B ion chamber linear output and log rate signals normalized
to their pre-trip values and displayed over 1 sec
SDS1-initiated trip from 60% of F.P. in
Darlington Unit 1, on August 28, 1995

SDS2 CHANNEL J RUNDOWN SIGNALS – 1 sec scale

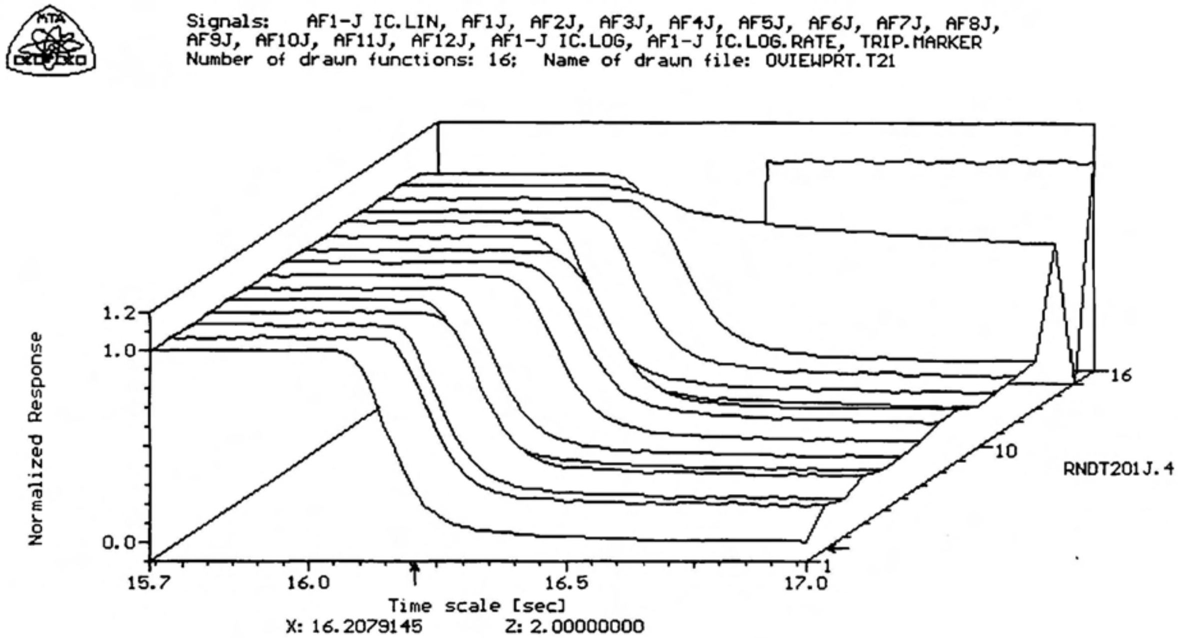

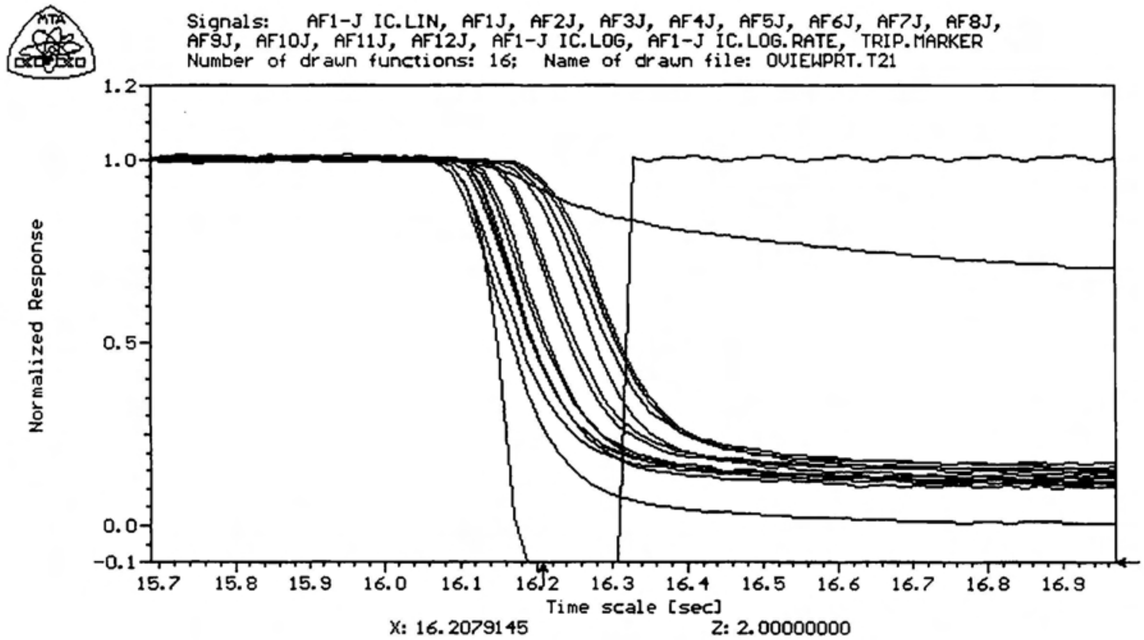

Figure 2. Rundown response signals of SDS2-J ICFDs (AF-1J through AF12J), SDS2-J ion chamber linear, log, log rate output and trip marker signals normalized to their pre-trip values and displayed over 1 sec. SDS2-initiated trip from 60% of F.P. in Darlington Unit 4, on August 23, 1996

SDS2 CHANNEL J RUNDOWN SIGNALS – 1 sec scale

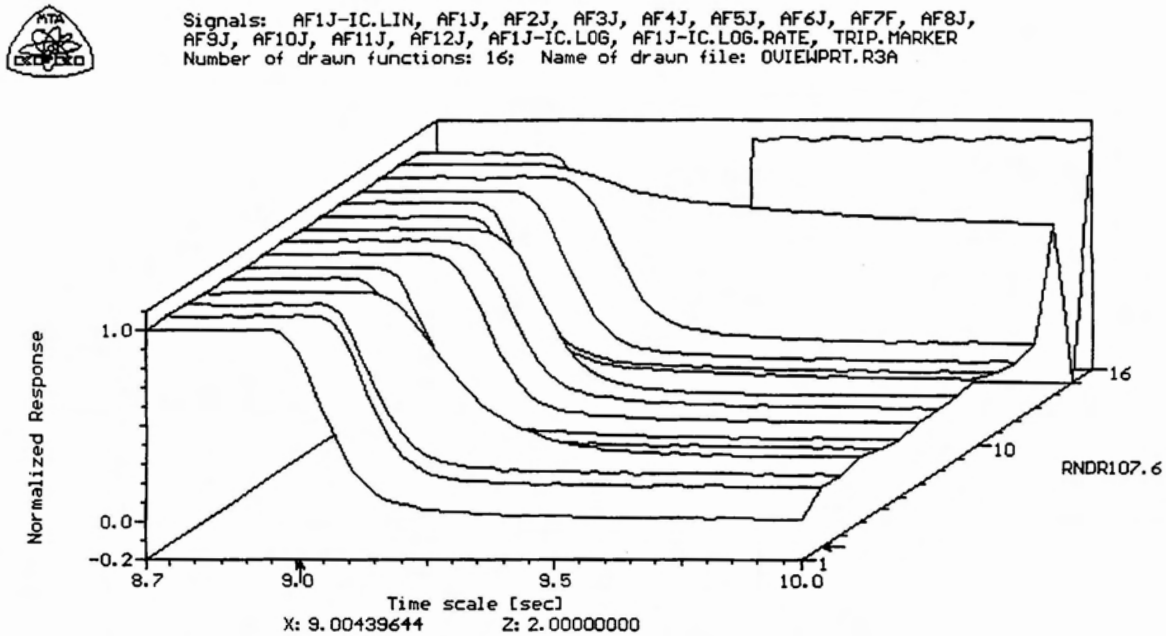

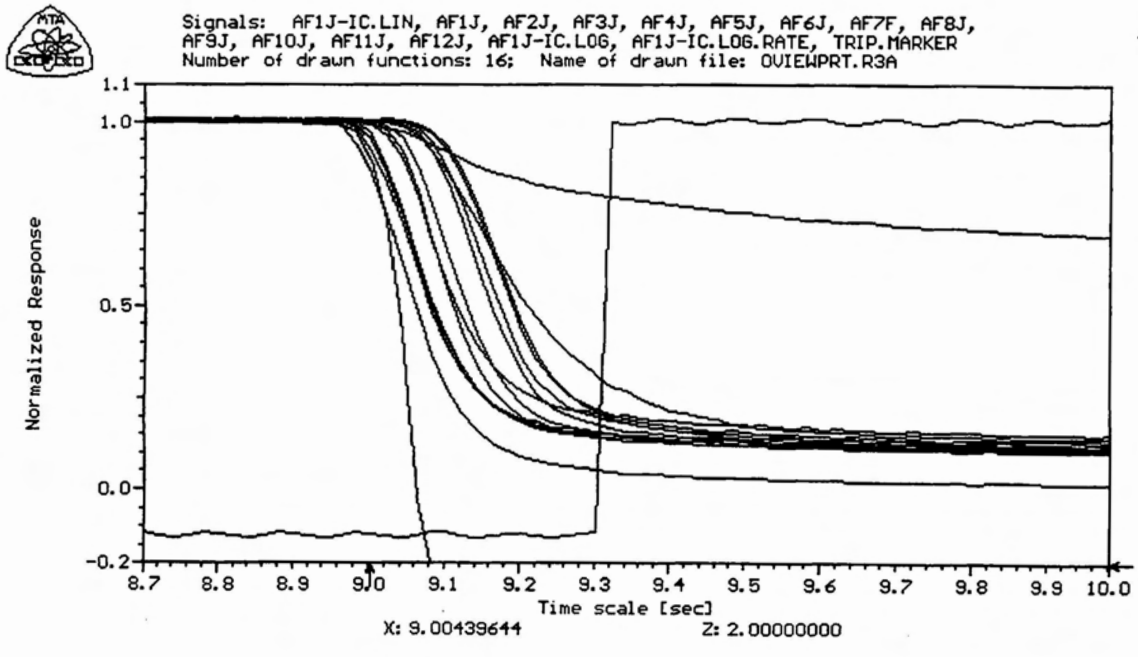

Figure 3. Rundown response signals of SDS2-J ICFDs (AF-1J through AF12J), SDS2-J ion chamber linear, log, log rate output and trip marker signals normalized to their pre-trip values and displayed over 1 sec. SDS2-initiated trip from 60% of F.P. in Darlington Unit 2, on November 18, 1995

APPENDIX A

DERIVING DETECTOR PROMPT FRACTION FROM RUNDOWN MEASUREMENT

In the time domain, the detector voltage signal $V_D(t)$ is modelled via the convolution of the time dependent flux, $\Phi(t)$, and the detector impulse response function, $h(t)$. The latter comprises the prompt fraction p and the N delayed components with time constant τ_n and relative magnitude k_n, respectively

$$h(t) \quad = \quad p\,\delta(t) \quad + \quad \sum_{n=1}^{N} \frac{k_n}{\tau_n} \exp(-t/\tau_n) \tag{1}$$

where $\delta(t)$ is the Dirac-delta function, and $p + \sum_{n=1}^{N} k_n = 1$.

The detector voltage is

$$V_D(t) \quad = \quad C_D \int_{-\infty}^{t} h(t - t')\,\Phi(t')\,dt' \quad + \quad V_B \tag{2}$$

where C_D is the product of the detector sensitivity factor and the gain of the station amplifier converting current to voltage, and V_B is a constant voltage off-set measured at zero power. In Darlington, the zero-power output voltage of the ICFD and ion chamber station amplifiers is 0.5V. In Pickering-B, this off-set voltage is zero for ICFDs and 0.1V for the ion chambers. The actual off-set V_B may vary from signal to signal because of the possible bias in station hardware and data acquisition electronics. The residual off-set voltage of the linear ion chamber signal is measured 12 hours after the shutdown, while the data acquisition system is still connected. The deviation between the zero off-set of different data acquisition channels is in the range of ± 10mV, or $\pm 0.2\%$ of the monitored voltage range. This uncertainty can result in a $\pm 0.5\%$ bias in the estimated prompt fraction.

Equations (1) and (2) yield

$$V_D(t) \quad = \quad C_D \left(p\,\Phi(t) \quad + \quad \sum_{n=1}^{N} \frac{k_n}{\tau_n} \int_{-\infty}^{t} \Phi(t') \exp\left(-\frac{t - t'}{\tau_n}\right) dt' \right) + V_B \tag{3}$$

Let us assume that before the trip the static flux was Φ_0 at the location of detector D, and the reactor trip occured at $t = 0$, and the flux decreased linearly to a constant level of $\Phi_1 < \Phi_0$, over a time period of T after the trip:

$$\Phi(t) = \begin{cases} \Phi_0, & \text{for } t < 0 \\ \Phi_0 - \frac{\Phi_0 - \Phi_1}{T}\,t, & \text{for } 0 < t < T \\ \Phi_1, & \text{for } T < t. \end{cases} \tag{4}$$

Rundown measurement at Ontario Hydro's CANDU stations showed that in SDS1-initiated trips (shut-off rods dropped) the ICFD and ion chamber signals quickly drop from the pre-trip values to a low value in 1 sec. In SDS2-induced trips (poison injection) the transition period is even shorter: the signals drop to a low value in 0.4 sec. Therefore, $T = 1$ sec is a reasonable assumption in numerical calculation. The SDS1/RRS and SDS2 ion chambers, located on the north and the south sides of the calandria, showed similar responses to reactor shutdown, in terms of time T and the relative signal drop Φ_1/Φ_0.

After inserting Equation (4) into Equation (3), for $t > T$

$$V_D(t) = C_D \left(\Phi_1 \quad + \quad (\Phi_0 - \Phi_1) \sum_{n=1}^{N} k_n \exp\left(-\frac{t}{\tau_n}\right) \frac{\exp\left(\frac{T}{\tau_n}\right) - 1}{\frac{T}{\tau_n}} \right) + V_B \tag{5}$$

Using the pre-trip equation $V_D(0) = C_D\,\Phi_0 + V_B$, the prompt fraction $p = 1 - \sum_{n=1}^{N} k_n$ is expressed as a function of the measured detector voltage signal, $V_D(t)$ for $t > T$

$$p = \left(1 - \frac{V_D(t) - V_B}{V_D(0) - V_B}\right)\left(1 - \frac{\Phi_1}{\Phi_0}\right)^{-1} - \sum_{n=1}^{N} k_n \left(1 - \exp\left(-\frac{t}{\tau_n}\right)\frac{\exp\left(\frac{T}{\tau_n}\right) - 1}{\frac{T}{\tau_n}}\right) \tag{6}$$

where $(V_D(t) - V_B)/(V_D(0) - V_B)$ represents the relative drop in detector voltage after the shutdown, while Φ_1/Φ_0 is the relative drop in flux at the location of the in-core detector. The detector signal $V_D(t)$ is continuously recorded during the rundown. If t is chosen such that $T < t \ll \tau_n$ for all delayed components, then each term in the above sum is close to zero.

Assumption #1: For time instant t satisfying $T < t \ll \min\{\tau_n\}_{n=1}^{N}$

$$\sum_{n=1}^{N} k_n \left(1 - \exp\left(-\frac{t}{\tau_n}\right)\frac{\exp\left(\frac{T}{\tau_n}\right) - 1}{\frac{T}{\tau_n}}\right) \ll 1 \tag{7}$$

that is

$$p \approx \left(1 - \frac{V_D(t) - V_B}{V_D(0) - V_B}\right)\left(1 - \frac{\Phi_1}{\Phi_0}\right)^{-1} \tag{8}$$

Assumption #1 introduces an error in the prompt fraction estimation, whose upper limit can be determined in a conservative calculation of the sum in Eq. (7) by setting $\tau_n = \min\{\tau_i\}_{i=1}^{N}$ for all delayed components. This would change the calculated prompt fraction in Eq. (6) by 1 %, that is, by omitting the summation, the effective prompt fraction of Inconel ICFDs (SDS1/RRS) would decrease by less than 1%, and it would increase by less than 1% for Platinum-clad Inconel ICFDs (SDS2).

Assumption #2: The relative flux drop Φ_1/Φ_0, (after/before the trip), at any detector location is represented by the relative signal drop of the ion chamber signal $(V_{ICH}(t) - V_{B'})/(V_{ICH}(0) - V_{B'})$. This is strictly true only in point kinetic reactors. In reality, the relative flux drop depends on the detector location, since the flux shape after the trip is different from the pre-trip flux shape. The after-trip flux shape is more uniform. It can be shown that by assuming a $\pm 15\%$ variation in the pre-trip static flux at the detector locations and a uniform flux shape after the trip, the application of Assumption #2 introduces a variation of $\pm 1.5\%$ in the effective prompt fraction.

With Assumptions #1 and #2, the prompt fraction of any in-core flux detector is approximated by the measured time series of the detector and the ion chamber signals at time t satisfying $T < t \ll \min\{\tau_n\}_{n=1}^{N}$:

$$p \approx \left(1 - \frac{V_D(t) - V_B}{V_D(0) - V_B}\right)\left(1 - \frac{V_{ICH}(t) - V_{B'}}{V_{ICH}(0) - V_{B'}}\right)^{-1} \tag{9}$$

Assumptions #1 and #2 lead to a simple interpretation of Equation (9): the prompt fraction of the ICFD is approximated with the ratio of the relative drop after the trip in the ICFD and the ion chamber (100% prompt reference signal).

Better statistics is obtained if the post-trip signals are averaged over a time interval (t_1, t_2) satisfying $T < t_1, t_2 \ll \min\{\tau_n\}_{n=1}^{N}$:

$$p \approx \left(1 - \frac{\overline{V_D(t_1, t_2)} - V_B}{\overline{V_D(0)} - V_B}\right)\left(1 - \frac{\overline{V_{ICH}(t_1, t_2)} - V_{B'}}{\overline{V_{ICH}(0)} - V_{B'}}\right)^{-1} \tag{10}$$

where

$$\overline{V_D(t_1,t_2)} = \frac{1}{(t_2-t_1)}\int_{t_1}^{t_2} V_D(t)\,dt$$

and

$$\overline{V_{ICH}(t_1,t_2)} = \frac{1}{(t_2-t_1)}\int_{t_1}^{t_2} V_{ICH}(t)\,dt$$

$\overline{V_D(0)}$ and $\overline{V_{ICH}(0)}$ are the averaged signal values measured before the trip.

Typical values for the time interval are $t_1 = 2.5$sec and $t_2 = 3.5$sec. Experience showed that the calculated prompt fraction is not very sensitive to the actual values of t_1 and t_2, provided that $T < t_1 < t_2 \ll \min\{\tau_n\}_{n=1}^{N}$.

Equation (10) gives an average value for the prompt fraction based on the average values of (1) the ICFD signal before the trip, (2) the ICFD signal 3 sec after the trip, (3) the ion chamber signal before the trip, and (4) the ion chamber signal 3 sec after the trip. The relative standard deviation of the prompt fraction can be calculated as the sum of the relative standard deviations of the above four components.

Since

$$p = \left(\frac{\overline{V_D(0)} - \overline{V_D(t_1,t_2)}}{\overline{V_D(0)} - V_B}\right)\left(\frac{\overline{V_{ICH}(0)} - \overline{V_{ICH}(t_1,t_2)}}{\overline{V_{ICH}(0)} - V_{B'}}\right)^{-1} \tag{11}$$

the relative standard deviation of p (uncertainty) can be calculated directly from the relative standard deviations of the measured time series

$$\frac{\sigma(p)}{p} = \frac{\sigma(\overline{V_D(0)} - V_D(t))}{\overline{V_D(0)} - V_D(t)} + \frac{\sigma(V_D(0))}{\overline{V_D(0)} - V_B} + \frac{\sigma(\overline{V_{ICH}(0)} - V_{ICH}(t))}{\overline{V_{ICH}(0)} - V_{ICH}(t)} + \frac{\sigma(V_{ICH}(0))}{\overline{V_{ICH}(0)} - V_{B'}} \tag{12}$$

where

$$\frac{\sigma(V_D(0))}{\overline{V_D(0)} - V_B}$$

is the relative standard deviation of ICFD signal fluctuations before the trip,

$$\frac{\sigma(\overline{V_D(0)} - V_D(t))}{\overline{V_D(0)} - V_D(t)}$$

is the relative standard deviation of the fluctuations in the ICFD signal drop after the trip over the time interval [2.5 sec, 3.5 sec],

$$\frac{\sigma(V_{ICH}(0))}{\overline{V_{ICH}(0)} - V_{B'}}$$

is the relative standard deviation of the Ion Chamber signal fluctuations before the trip,

$$\frac{\sigma(\overline{V_{ICH}(0)} - V_{ICH}(t))}{\overline{V_{ICH}(0)} - V_{ICH}(t)}$$

is the relative standard deviation of the fluctuations in the Ion Chamber signal drop after the trip over the time interval [2.5 sec, 3.5 sec].

APPENDIX B

EFFECTIVE PROMPT FRACTIONS DERIVED FROM MEASUREMENTS – CHANNEL J

Table 1. Prompt Fraction of Darlington Unit 4 SDS2 channel J Platinum-clad Inconel In-Core Flux Detectors Derived from SDS2-initiated Rundown Curves

SDS2-J	**Prompt**	**IR***	**DC**	%	%	%	%
Detec.	%	$M\Omega$	**pre-trip**	**3 s**	**30 s**	**300 s**	**12 hr**
1J HFD1-RE2J	88.1 ±0.4	–	2.51 v	12.1	10.3	8.9	1.5
2J HFD2-RE1J	91.1 ±0.4	–	2.47 v	9.1	7.7	6.8	1.4
3J HFD2-RE3J	86.1 ±0.4	–	2.37 v	14.1	12.2	10.6	1.7
4J HFD4-RE1J	90.5 ±0.4	–	2.43 v	9.7	8.1	6.7	1.8
5J HFD5-RE2J	90.0 ±0.4	–	2.88 v	10.2	8.2	6.7	2.2
6J HFD5-RE3J	88.3 ±0.4	–	2.68 v	11.9	10.5	9.2	1.4
7J HFD6-RE4J	85.6 ±0.3	–	2.47 v	14.6	13.4	12.2	2.5
8J HFD7-RE4J	83.3 ±0.3	–	2.28 v	16.9	16.1	15.2	2.0
9J HFD9-RE2J	90.8 ±0.4	–	2.61 v	9.4	7.6	6.3	1.8
10J HFD11-RE1J	90.2 ±0.5	–	2.43 v	10.0	8.0	6.4	2.4
11J HFD11-RE2J	87.5 ±0.4	–	2.66 v	12.7	11.3	9.8	2.0
12J HFD11-RE4J	86.2 ±0.4	–	2.36 v	14.0	13.6	12.7	2.5
13J HFD12-RE1J	87.2 ±0.4	–	2.27 v	13.0	10.7	8.9	2.4
14J HFD13-RE2J	86.7 ±0.4	–	2.42 v	13.4	11.5	10.1	2.8
15J HFD14-RE2J	92.3 ±0.4	–	2.38 v	7.8	6.5	5.6	1.7
16J HFD14-RE3J	87.5 ±0.4	–	2.48 v	12.6	10.6	9.2	3.2
17J HFD14-RE6J	81.8 ±0.4	–	2.38 v	18.3	16.8	15.2	2.5
ICH.-J	100.0 ±0.2	N/A+	2.06 v	0.2	0.1	0.0	0.0

* (IR not available yet)

\+ (SDS2-J ion chamber linear output)

The SDS2-J ICFD signals started to decrease 420 msec after the SDS2 trip was initiated. The power step recorded by the channel J ion chamber was completed in additional 400 msec. The normalized voltage values shown in Table 1 at 3 sec, 30 and 300 sec were averaged over an interval of 1 sec (50 samples). The values shown at 12 hours after the trip were averaged over an interval of 4 sec.

The error band indicates the $\pm\sigma$ statistical uncertainty of the prompt fraction estimate in Equation (1), caused by the fluctuations of ICFD and ion chamber readings. Since the statistical distribution of the ratio in Equation (1) is not Gaussian, the usual confidence level of 99.73% associated with the $\pm 3\sigma$ confidence interval is not valid in this case. A conservative confidence level still can be given: by applying the Tchebycheff Inequality theorem of random variables with unkown statistical distribution, we found that the probability of having the true prompt fraction within the $\pm 3\sigma$ error bound is higher than 90%, regardless of the actual statistical distribution of the prompt fraction calculated in Equation (1). The 90% inclusion probability limit is a conservative value, the actual accuracy of the estimate of the prompt fraction may be much better.

The above statistical uncertainties can be estimated accurately from the fluctuations of the measured signals. However, there are two more sources of uncertainties affecting the calculated prompt fraction, which cannot be estimated directly from the measurements: (1) the effect of spatial dependency of the power step and the assumption on the post-trip flux shape can cause a systematic deviation in the EFP, in the range of ±1.5% (see Appendix A), (2) further bias could be introduced by the uncertainty of the zero off-set of the data acquisition channels (±10 mvolt), resulting in a ±0.5% uncertainty in the calculated EFP.

Table 2. Time difference measured between the Trip Marker of SDS2-initiated trip and detectors signal reaching 50% of their pre-trip value

Amp. ID.	Detec. ID	Time* msec	Coord. Column	Coord. Row	Prompt %
AF-1J	ICH.LIN-J	530	—	—	100.0 ± 0.2
AF-4J	HFD4-RE1J	540	2 - 5	H - J	90.5 ± 0.4
AF-5J	HFD5-RE2J	555	6 - 9	H - J	90.0 ± 0.4
AF-10J	HFD11-RE1J	560	3 - 6	Q - R	90.2 ± 0.5
AF-2J	HFD2-RE1J	565	8 - 11	E - F	91.1 ± 0.4
AF-9J	HFD9-RE2J	570	6 - 9	Q - R	90.8 ± 0.4
AF-13J	HFD12-RE1J	575	6 - 9	T - U	87.2 ± 0.4
AF-1J	HFD1-RE2J	575	11 - 14	E - F	88.1 ± 0.4
AF-15J	HFD14-RE2J	585	9 - 12	T - U	92.3 ± 0.4
AF-16J	HFD14-RE3J	605	11 - 14	T - U	87.5 ± 0.4
AF-3J	HFD2-RE3J	605	14 - 17	E - F	86.1 ± 0.4
AF-14J	HFD13-RE2J	610	11 - 14	T - U	86.7 ± 0.4
AF-11J	HFD11-RE2J	610	12 - 15	Q - R	87.5 ± 0.4
AF-6J	HFD5-RE3J	635	18 - 21	H - J	88.3 ± 0.4
AF-7J	HFD6-RE4J	655	20 - 23	H - J	85.6 ± 0.3
AF-8J	HFD7-RE4J	665	21 - 24	M - N	83.3 ± 0.3
AF-17J	HFD14-RE6J	670	19 - 22	T - U	81.8 ± 0.4
AF-12J	HFD11-RE4J	670	21 - 24	Q - R	86.2 ± 0.4

* between trip marker and 50% of pre-trip value

Table 2 show the time difference measured between the Trip Marker of SDS2-initiated trip and channel J detector signals reaching 50% of their pre-trip value as a function of detector location. The time delay follows a south-to-north pattern due to the propagation of poison inside the injection nozzle. Variation in delay time may be caused by the additional time required for poison propagation in the moderator. The accuracy of the time scale is ±5 msec.